Experiments and Direct Simulations of Fluid Particle Motions

Howard H. Hu, Daniel D. Joseph
Department of Aerospace Engineering and Mechanics
University of Minnesota, Minneapolis, MN55455

Antonio F. Fortes
Department of Mechanical Engineering, University of Brasilia
70910 - Brasilia - DF, Brasil

Abstract

This paper and the accompanying video segment show how the motions of sedimenting particles may be simulated by direct computations based on the Navier-Stokes equations and the particles equations of motion. Sedimenting and fluidized particles are confined by closely spaced walls to move essentially in two dimensions under forces determined by three-dimensional motions of the fluidizing liquids. Attention is confined to the case when there are only few particles, not more than four. The experiments and simulations give rise to deterministic dynamics, to equilibrium positions and steady flows, to Hopf bifurcation and wavy fall trajectories and to more chaotic motions. It is shown that long bodies always turn to put their broadside perpendicular to the stream. The same mechanism which causes long bodies to turn broadside-on causes spherical bodies, which come into contact by wake interactions, to tumble, giving rise to a flow induced anisotropy in which across stream arrangements are favored. The numerical simulation, unlike the experiments, is strictly two-dimensional, but many of the observed features of the experiments are predicted by the simulation.

The video segment on which this paper is based is a stand alone document. The paper gives additional information which is not conveniently expressed in a video format.

This work was supported by the National Science Foundation, the Department of Energy and the Army Research Office, Mathematics. Numerical simulations were done under grants from Minnesota Supercomputer Institute and Army High Performance Computing Research Center (AHPCRC).

The nonlinear properties of flow of a few fluidized particles can be discussed in two different theoretical frameworks:

1. A natural frame for our studies of the motions of particles in fluids is in terms of the principle of hydrodynamics, the roles played by stagnation points, separation points, vortex shedding, wakes, turning couples on long bodies and bodies in momentary contact. For example, we can determine the nature of the forces in two-dimensional simulations which presumably drive spheres to the center of a two-dimensional bed used in experiments. This kind of deterministic dynamics may play a role in lubricated transport of solid particles.

2. A different and equally illuminating way to discuss the motion of particles is in terms of bifurcation theory and dynamical systems. For example, take the case of a single sphere sedimenting from rest in a viscous liquid between planes. At small Reynolds numbers there is no vortex shedding and the sphere falls in a straight line under gravity, and we found that the channel center is an equilibrium, apparently globally stable since no matter how off center the sphere is initially, it will eventually drift to the center. At higher Reynolds numbers, the central position of equilibrium loses stability and undergoes a Hopf bifurcation in which the center is no longer an equilibrium. The cause of the loss of stability of steady flows is vortex shedding. We get a periodic solution in which the sphere oscillates with the same frequency as the trajectory waves around its off-center mean position of equilibrium. When the flow goes turbulent it is possible that the motion of the sphere will be chaotic.

There is a difference between the experiments in two-dimensional beds and the numerical simulations which are confined strictly to two dimensions. The experiments were done in a channel whose walls were separated by small gap slightly lager than the smallest radius of the particle. In this way the centers of mass of the particles were confined to move more or less in two dimensions, but the flow around the particle is three-dimensional. The particle diameter in the experiments on sedimentation were about 1/4 inch, the fluid was aqueous glycerin, 50% water. The experiments on drafting, kissing and tumbling in a fluidized bed were also carried out in a 50/50 glycerin water mixture using 1/2 inch diameter spheres.

The numerical simulation is based on an extension of the code POLYFLOW which was constructed by Howard Hu and is reported in a paper by Hu, Joseph and

Crochet [1992]. Some details of this code are given in a appendix to this paper. The simulation is like a macroscopic molecular dynamics based on correct equations, the Navier-Stokes equations for the fluid and the particles equations of motion for the solids using forces computed from the stresses induced by the fluid motion.

A comparison of the direct strictly two-dimensional numerical solution with the experiments in two-dimensional beds shows that kissing interactions are relatively suppressed in the simulation. This may be a physically correct result reflecting a genuine difference between two and three dimensions. Kissing bodies seen in two dimensions have a line contact; in three dimensions kissing spheres have a point contact. The numerical code cannot handle situations in which particles touch; when this happens the simulation stops. In some cases the simulations did stop, but not in the ones seen in the video.

We need to know if and how two-dimensional simulations represent the two-dimensional motions of bodies in three dimensions. Perhaps in certain situations the simulations represent features of the experiment, but at a different Reynolds number.

There are four different effects which are clearly developed in the video segment: turning couples on long bodies; drafting, kissing and tumbling; the equilibrium positions and stability and bifurcation of particle motions.

A four to one channel means that the width of the channel is four times the gap; the eight to one channel is twice as wide. In the experiments the center of the channel is an attractor for single particles, long bodies and spheres. Apparently the center is a globally attractor since no matter how or where the particles are dropped, they appear always to drift toward the center. At low Reynolds numbers, in the experiments the center is an equilibrium; the flow is steady. This is seen clearly in the opening segment of the video where a cylinder whose length is twice its diameter settles steadily in the channel center at Reynolds number of 57. When the Reynolds number is increased to 350 steady flow is unstable; it gives way to a periodic solution which can be viewed as arising from a Hopf bifurcation. The center is still a mean position of equilibrium, but the particle rocks and the trajectory waves around the mean position of equilibrium in lock step with the periodic shedding of vortices from points of separation on the long body.

The broadside-on orientation of the long particle is a robust feature. No matter how the particle is dropped it will very quickly put its broadside perpendicular to the

stream. The natural orientation of long bodies is a key element in determining the kind of flow-induced anisotropic structures which develop in beds of many spherical particles.

The robust tendency for long bodies to settle with their broadside perpendicular to the stream is also evident in the direct simulation of a falling 2/1 ellipse. The ellipse settles stably and steadily in the 8/1 channel at a Reynolds number of 17. The center is an equilibrium and the broadside-on configuration is robustly stable. At this Reynolds number and at a Reynolds number of 60 the center of the channel is an attractor and no matter how or where the ellipse is dropped it will turn its broadside into the stream and drift to the channel center. The steady fall of the ellipse seen at *R*e=17 gives way at *Re*=60 to a periodic solution driven by vortex shedding which can be seen clearly in the simulation. The panel on the left of the simulation shows the streamlines; the panel on the right shows the vorticity and the center panel shows the dynamic pressure.

The dynamics of the sedimenting ellipse started from rest can be generally understood as being produced by turning at the stagnation points on an airship in potential flow (figure 1).

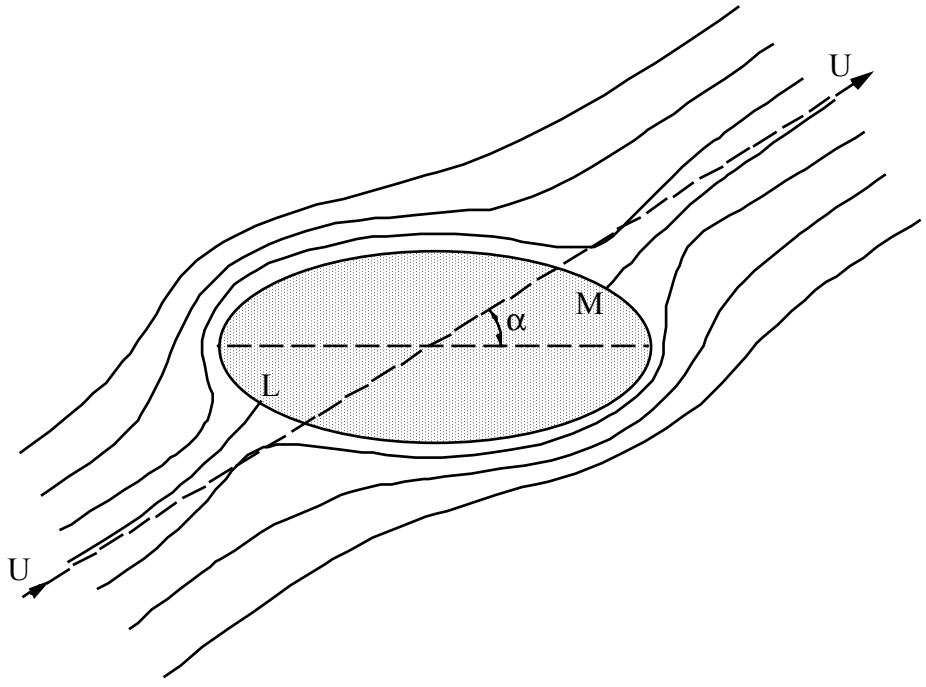

Figure 1. The high pressures at the stagnation points cause the airship to turn its broadside to the stream, to stall.

Some experiments were done by C. Sioutas [1989]. Long round cylinders of diameter 0.5 cm and length 1 cm and 2.5 cm were dropped in water filling the gap between glass plates. The gap size was slightly larger than 0.5 cm so that the motion of the cylinders was confined to a plane. The cylinders were heavier than water. The flow was steady and the cylinders settled broadside-on when the Reynolds number based on 0.5 cm was less than 57. The next data point at Re=211 was in strong unsteady flow, oscillating around broadside-on. Hence the critical Re is between 57 and 211. This compares with the critical values of 40 for flow over a cylinder. The Strouhal number is nearly constant, about 0.21 for Reynolds numbers from about 300 to 200,000. These same frequencies are observed in two-dimensional flow across cylinders, a very different flow. We regard the experiments of Sioutas as preliminary. More and better experiments are needed to determine the response of long particles in three regimes: (i) Stokes flow, (ii) steady nonlinear flow with $Re<Rc$ where Rc is to-be-determined Reynolds number probably near 57, (iii) the post-stability regime where the rocking frequency is a quantity of central interest.

Of course the sedimenting ellipse shown in the video is not in a potential flow. Nevertheless a careful monitoring of high (yellow) and low (red and blue) pressures on the ellipse show a very similar dynamics. The exact balance of forces which cause the long body to turn broadside-on are contained in details which can be recovered from simulation. The true dynamics are better represented by figure 2 and figure 3, from the simulation than by figure 1 for potential flow. The stagnation pressure still operates on the front side of the ellipse, but there is a "dead water" region on the back side which can have large negative pressures, even larger than the positive pressures at the front stagnation point. These large negative pressures occur in pairs at the separation points on left and right of the back side of the ellipse as shown in figure 3 and they give rise to a couple which control the turning of the ellipse. The "potential flow" stagnation pressure at the front side controls the stability of the orientation of the ellipse which always has, on the average, its broadside perpendicular to the stream.

The rocking amplitudes of the ellipse in the simulation at Re=60 are much greater than the rocking amplitude of the 2/1 particles in the experiments at Re=350. It could be argued that the vortex shedding which produces this rocking should be greatly different in two than in three dimensions. The vortices must be shed from a generator of a cylinder in two dimensions but could come off a region near a point in three dimensions.

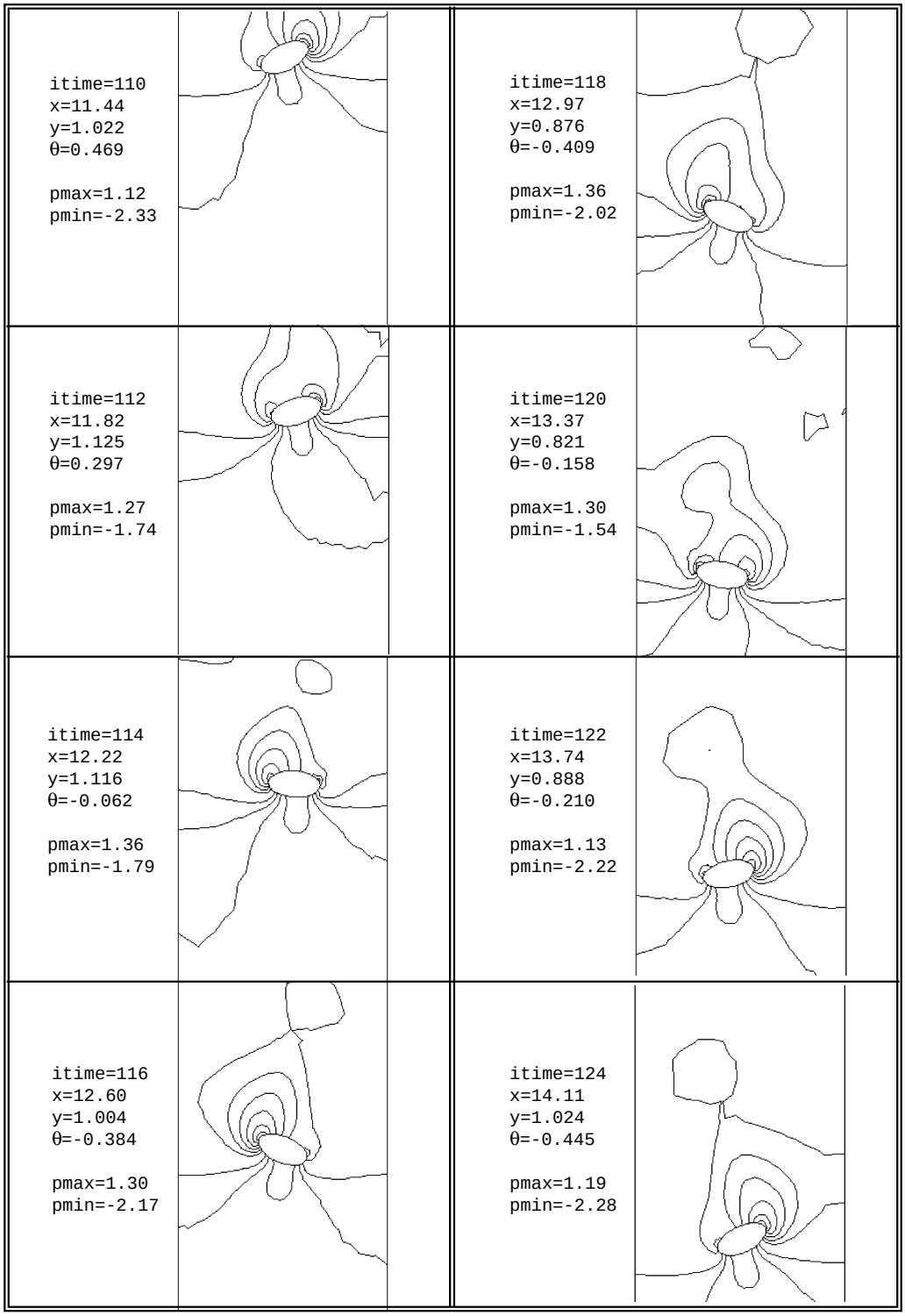

Figure 2. Pressure contour plots for a sedimenting ellipse during a cycle of rocking at *Re*=60. (x,y,θ) indicates the position of the ellipse. *pmax* and *pmin* are the maximum and minimum values of the dynamic pressure at each instant. From pmin to pmax there are nine equally spaced iso-pressure lines in each plot with high pressure in front.

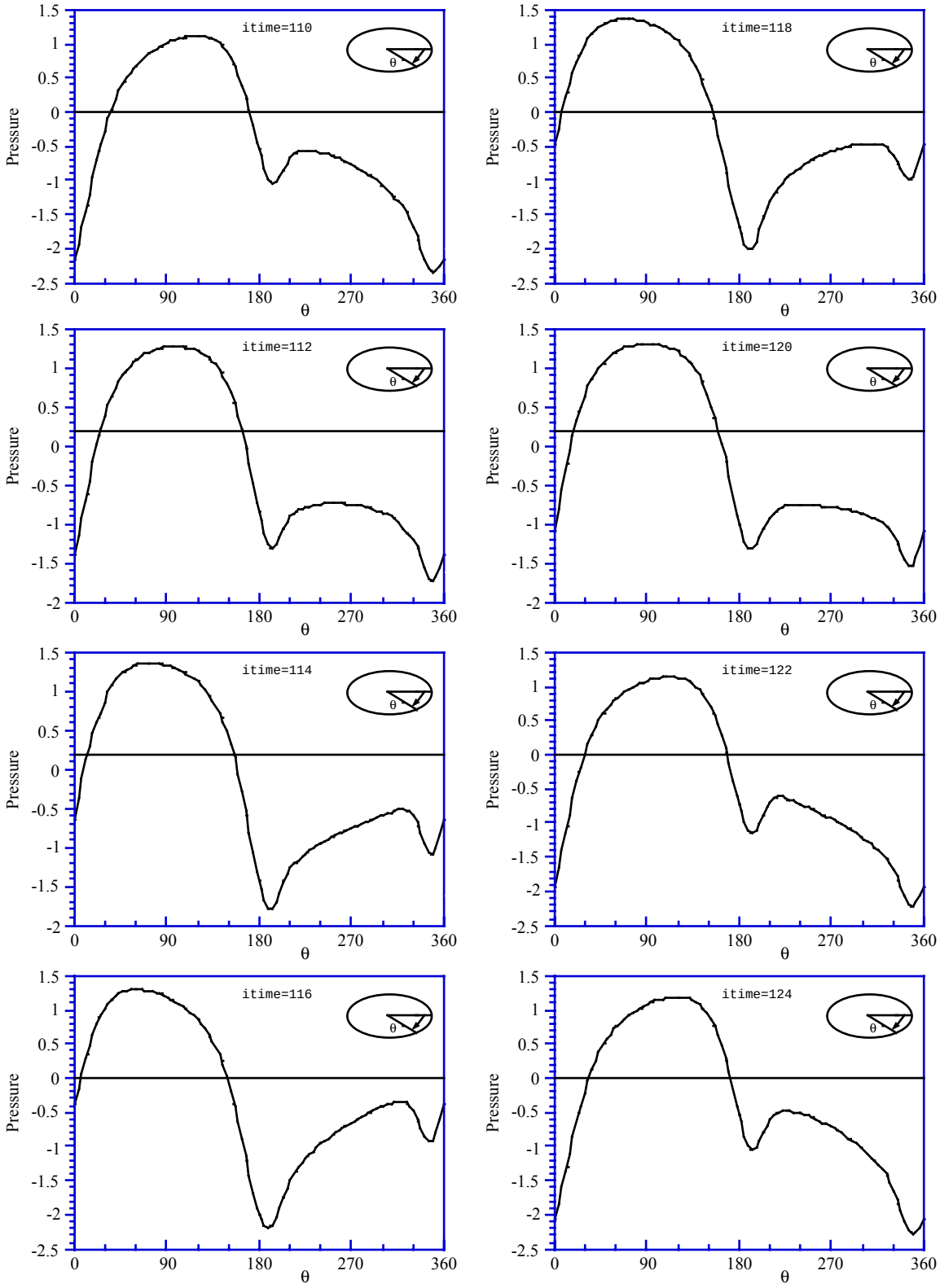

Figure 3. Pressure distribution on the surface of the ellipse for the times shown in figure 2. The two peaks of negative pressure on the back of the ellipse control the turning of the ellipse.

Another point of difference between experiments in two-dimensional beds and simulations in two dimensions occurs in the equilibrium positions of a settling sphere in the two-dimensional bed and a settling circular particle in two dimensions. In the experiments at modest Reynolds numbers, even thousands, the center is a mean position of equilibrium. In the simulation it appears that the channel center is an equilibrium when Re=40 and the fall of the circular particle is steady. At Re=70 the fall is not steady; vortex shedding gives rise to a periodic solution whose mean position of equilibrium is off center.

Local nonlinear dynamics associated with wakes and turning couples on long bodies give rise to scenario which can be described as "drafting, kissing and tumbling". This scenario is very robust and appears to control the dynamics of particles in suspension at all but the smallest Reynolds numbers. There is a wake with low pressure at the back of fluidized or sedimenting sphere in three dimensions or circular cylinder in two dimensions. A second sphere will be sucked into the wake of the first, like debris behind a fast moving car. This is called drafting, after the well-known bicycle racing strategy which is based on the same principle. Drafting spheres are sucked into contact; they kiss. Kissing spheres form a long body which is unstable when its line of centers is along the stream. The same couples which force a long body to float broadside-on cause kissing spheres to tumbling. Tumbling spheres induce anisotropy of suspended particles since on the average the line of centers between spheres must be across the stream. If it is not across the stream the spheres will draft, kissing and tumble again, or else they may not interact. This escape scenario is in evidence at the end of the simulations of interacting circular cylinders at Re=40 and Re=70. The interactions of spheres in the two-dimensional bed seems to be more persistent though escape scenario can be seen in experiments as well.

Very remarkable steady flows of fluidized 6.35 mm diameter spheres in a fluidized bed with a 12.7 mm gap were observed in experiments by Fortes and Joseph [1992]. Stable, steady nested wake clusters were observed in the range of Reynolds number $22<Re<43$. These arrangements are shown in figures 4-6. They are unstable and they draft, kiss and tumble when the Reynolds number is smaller than 22 or larger than 43. All the observed arrangements are essentially planar, as the spheres rotate and position themselves with centers in a vertical plane that is not in the center between the two walls of the apparatus. We interpret this sideward displacement as a Segre-Silberberg effect. The clusters always have a higher drag than a single particle, which means that the stable architectures occur at fluid velocities always greater than the individual terminal free falling velocities of spheres.

The arrangements shown in figure 5 and 6 are often seen in the migrating birds in flight. Maybe the arrangement used by birds is useful only for a certain range of speeds. Singh et al [1989], showed that a cross-stream array of fluidized cylinders equally spaced and all in a row was stable to different perturbations, but it is not yet known if these stable arrays, of Fortes & Joseph [1992], can be obtained from strictly two-dimensional dynamics simulations.

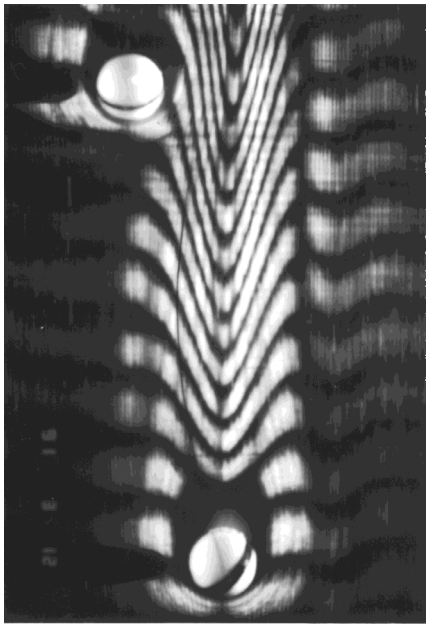

Figure 4. Visualization of the velocity profiles as a stably locked pair of Teflon sphere 6.35 mm diameter. *Re*=22.48. The fluidized spheres are in perfect equilibrium under weight and drag.

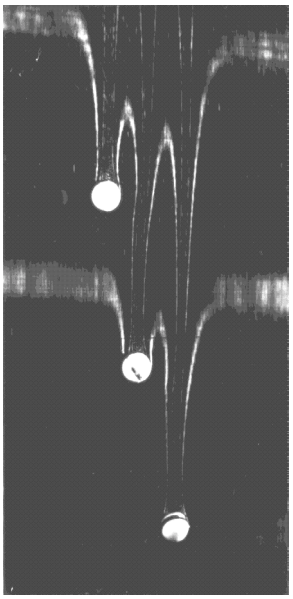

Figure 5. Three Teflon spheres locked together at *Re*=28.4, each at the edge of the wake of the preceding sphere. These staggered wake architectures are stable in the range $22<Re<43$.

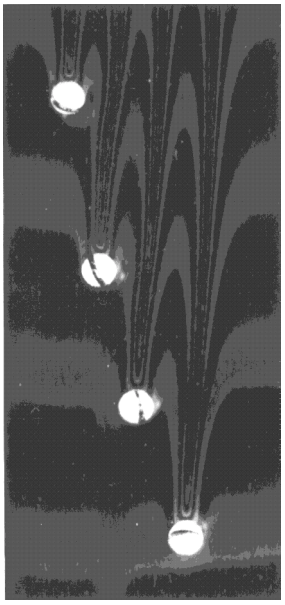

Figure 6. Four Teflon spheres locked together, each at the edge of the wake of preceding sphere. These staggered wake architectures are stable in a small range of Reynolds numbers. The nested wake structures resemble some formations which can be seen in migrating birds in flight.

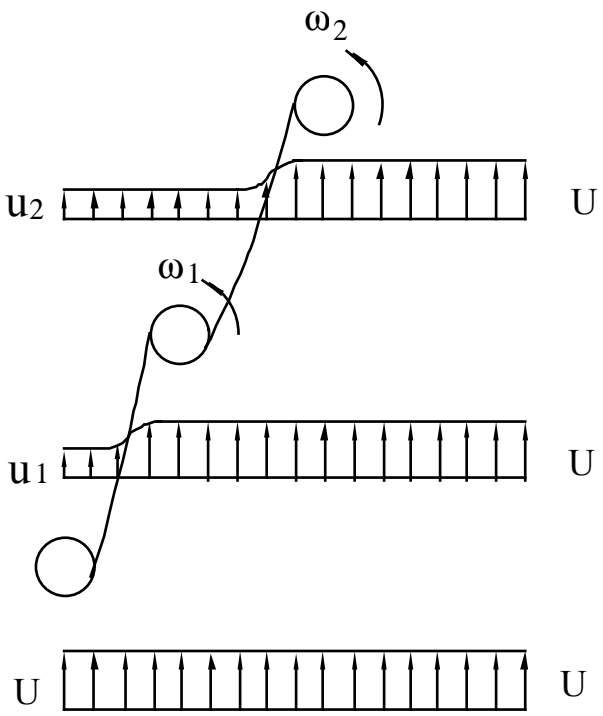

Figure 7. The wake architecture with three particles. The rotations ω_1 and ω_2 around axis normal to the walls are due to the velocity gradient of the wake and are such that $\omega_1 \leq \omega_2$. The upstream (bottom) sphere rotates more slowly.

References

Fortes, A., Joseph, D.D. (1992), Wake architectures in two-dimensional fluidization of spheres. Experiment and phenomenological description. *Proceedings of the joint DOE-NSF workshop on flow of particulates*, Oct. 1991.

Hu, H.H., Joseph, D.D. and Crochet, M.J. (1992), Direct simulation of fluid particle motions, *J. Theoretical and Computational Fluid Dynamics*, xx, 000-000.

Singh, P., Caussignac, Ph., Fortes, A., Joseph, D.D. and Lundgren, T.S. (1989), Stability of periodic arrays of cylinders across the stream by direct simulation, *J. Fluid Mech.* **205**, 553-571.

Sioutas, C. (1989), Strouhal frequencies of a single cylinder falling in water under gravity in plane motion between glass plates. Master paper, Department of Aerospace Engineering and Mechanics, University of Minnesota.

Appendix

The numerical results shown in the video were obtained with an Explicit–Implicit Scheme. At each time step the positions of the particles are updated explicitly, the velocities of the particles are determined implicitly (or iteratively), coupled with the solution of the flow. The iteration for the particle velocities is buried inside the nonlinear Newton iteration of the Navier–Stokes solver for an increased efficiency. The details of the scheme are described below.

Explicit–Implicit Scheme

(1). Initialization: $t_0=0$, $n=0$ (index for time step);
$\mathbf{u}(\mathbf{x}(t_0),0)=0$,
and $\mathbf{X}_i(t_0)=\mathbf{X}_{i0}$, $\mathbf{U}_i(t_0)=0$, $\mathbf{f}_i(t_0)=((\rho_s-\rho_f)/\rho_s, 0, 0)$, for $i=1,...,N$.

(2). Updating 1: select an appropriate time step Δt_{n+1},
$t_{n+1} = t_n+\Delta t_{n+1}$,
$\mathbf{X}_i(t_{n+1}) = \mathbf{X}_i(t_n) + \Delta t_{n+1}\, \mathbf{U}_i(t_n)$, for i =1,...,N,
$k=0$ (index for iteration),
initially update the particle velocities $\mathbf{U}_i^{(0)}(t_{n+1})$.

(3). Remeshing and Projection:

generate a new mesh $\mathbf{x}(t_{n+1})$ based on $\mathbf{X}_i(t_{n+1})$,
project velocity $\mathbf{u}(\mathbf{x}(t_n),t_n)$ to $\mathbf{u}(\mathbf{x}(t_{n+1}),t_n)$.

(4). One step Navier–Stokes iteration: $k = k+1$,

on the new mesh $\mathbf{x}(t_{n+1})$, with $\mathbf{u}(\mathbf{x}(t_{n+1}),t_n)$ as the initial condition and $\mathbf{U}_i^{(k-1)}(t_{n+1})$ as the boundary condition, perform *one* Newton iteration in the Navier–Stokes solver to get $\mathbf{u}^{(k)}(\mathbf{x}(t_{n+1}),t_{n+1})$, $p^{(k)}(\mathbf{x}(t_{n+1}),t_{n+1})$ and calculate $\mathbf{f}_i^{(k)}(t_{n+1})$.

(5). Updating 2:

$$\Delta\mathbf{U}_i^{(k)}(t_{n+1}) = -\mathbf{U}_i^{(k-1)}(t_{n+1}) + \mathbf{U}_i(t_n) + \Delta t_{n+1}\,\mathbf{f}_i^{(k)}(t_{n+1}),$$
$$\mathbf{U}_i^{(k)}(t_{n+1}) = \mathbf{U}_i^{(k-1)}(t_{n+1}) + \alpha\Delta\mathbf{U}_i^{(k)}(t_{n+1}), \quad \text{for } i=1,\ldots,N,$$

where α is a relaxation parameter.

(6). Convergence Test:

$$\varepsilon_1 = \|\Delta\mathbf{U}_i^{(k)}(t_{n+1})\|,$$
$$\varepsilon_2 = \|\mathbf{u}^{(k)}(\mathbf{x}(t_{n+1}),t_{n+1}) - \mathbf{u}^{(k-1)}(\mathbf{x}(t_{n+1})t_{n+1})\|.$$

If $(max(\varepsilon_1,\varepsilon_2) \geq \varepsilon)$ go to (4) , otherwise

$$\mathbf{U}_i(t_{n+1}) = \mathbf{U}_i^{(k)}(t_{n+1}), \quad \mathbf{f}_i(t_{n+1}) = \mathbf{f}_i^{(k)}(t_{n+1}),$$
$$\mathbf{u}(\mathbf{x}(t_{n+1}),t_{n+1}) = \mathbf{u}^{(k)}(\mathbf{x}(t_{n+1}),t_{n+1}),$$
$$p(\mathbf{x}(t_{n+1}),t_{n+1}) = p^{(k)}(\mathbf{x}(t_{n+1}),t_{n+1}).$$

(7). If the time t_{n+1} is less than T then $n := n+1$ and go to (2); otherwise stop.

In the above scheme, $\mathbf{X}_i$, $\mathbf{U}_i$ and $\mathbf{f}_i$ are the position, velocity and acceleration vectors of the particle i, $\mathbf{u}$ and p are the velocity and the pressure of the fluid and $\mathbf{x}(t_{n+1})$ represents the mesh nodes at time t_{n+1}.